Electronic Supplementary Information

Constructing Nanoneedle Arrays of Heterostructured RuO_2-Co_3O_4 with Tip-effect-induced Enrichment of Reactants for Enhanced Water Oxidation

Xu Zhang,[a] Junnan Song,[a]* Tongming Sun,[b] Minmin Wang,[b] Jinli Zhu,[b] Yang Yu,[c]* and Jiacheng Wang[a]*

[a] Zhejiang Key Laboratory for Island Green Energy and New Materials, Institute of Electrochemistry, School of Materials Science and Engineering, Taizhou University, Taizhou 318000, Zhejiang, China.

[b] College of Chemistry and Chemical Engineering, Nantong University, Nantong 226019, Jiangsu, China.

[c] School of Pharmaceutical Sciences, Taizhou University, Taizhou 318000, Zhejiang, China.

1. Experimental section

1.1 Chemicals

Cobalt nitrate hexahydrate ($Co(NO_3)_2·6H_2O$, AR), ruthenium (III) chloride hydrate ($RuCl_3·xH_2O$, 37%), urea (CH_4N_2O, AR), ammonium fluoride (NH_4F, AR), and ruthenium (IV) oxide (RuO_2) were purchased from Shanghai Aladdin Biochemical Technology Co. Ltd. All reagents were used directly without further purification.

1.2 Preparation of electrocatalysts

1.2.1 Preparation of RuO_2/Co_3O_4 on NF.

Before synthesis, nickel foam (NF) was treated ultrasonically in acetone, 1 M hydrochloric acid, deionized water, and ethanol for 10 minutes to enhance its hydrophilicity. Next, 0.58 g of $Co(NO_3)_2·6H_2O$, 0.3 g of NH_4F, and 0.6 g of CH_4N_2O were stirred in 40 mL of deionized water for 4 hours to form a uniform pink solution. This solution was then transferred to a 50 mL autoclave, and a piece of NF (2*3 cm^2) was fully immersed in the solution. The autoclave was sealed and heated at 120 °C for 9 hours. After cooling to room temperature, the NF containing the precursor was washed repeatedly with deionized water and dried in a vacuum oven at 60 °C for 12 hours to obtain CoCH. The resulting sample was heated to 350 °C at a rate of 5 °C per minute in an air atmosphere and held for 3 hours to obtain Co_3O_4. Co_3O_4 was then soaked for 9 hours in a 5 mg mL^{-1} $RuCl_3$ aqueous solution, followed by vacuum drying overnight at 60 °C and annealing for 2 hours in an air atmosphere at 320 °C. The final product was named RuO_2/Co_3O_4. The loading of Ru was adjusted by soaking in 5 mg mL^{-1} $RuCl_3$ aqueous solution for different times.

1.2.2 Preparation of RuO_2 on NF.

The commercial RuO_2 (5 mg) was dispersed into a mixture of 700 μL ethanol, 250 μL Isopropanol and 50 μL Nafion (5%), and the mixture was ultrasonicated for 30 min to form homogeneous ink. Then, a certain amount ink was loaded onto nickel foam and dried at room

temperature. The loading amount of RuO_2 on the 1*1 cm^{-2} NF was about 2.5 mg cm^{-2}, which was the same amount with the as-prepared electrocatalysts.

1.3 Characterization

Morphology and microstructure were observed using scanning electron microscopy (SEM, Hitachi S-4800) and transmission electron microscopy (TEM, Thermo Fisher Scientific Talos F200i). The dynamic contact angle was measured using an OCA20 instrument. The elements were analyzed by ICP-OES (inductively coupled plasma light emission spectrometry). X-ray powder diffraction (XRD, Bruker D8 Advance) was used to analyze the phase structure of the catalyst. The Bruker EMX-6/1 instrument was used to measure electron paramagnetic resonance (EPR) data and determine oxygen vacancies. The valence and surface atomic ratios of the catalysts were obtained using X-ray photoelectron spectroscopy (XPS, Shimadzu AXIS Supra+).

1.4 Electrochemical measurements

All electrochemical experiments were carried out using a three-electrode system in 1 M KOH, with $RuO_2Co_3O_4$/NF, carbon rod and Hg/HgO_2 electrodes as the working electrode, the opposition electrode and the reference electrode, respectively. The potential was modified to a reversible hydrogen electrode (RHE) by Nestor's equation ($ERHE = E_{Hg/HgO2} + 0.616V + 0.0591\times pH$). Linear scanning voltammetry (LSV) curves are obtained at a scanning rate of 1 mV S^{-1}. Electrochemical surface area (ECSA) is determined by measuring capacitance at scan rates of 2, 4, 6, 8, and 10 mV s^{-1}. Electrochemical impedance spectroscopy (EIS) measurements were performed in the frequency range 0.01 to 100 kHz with an AC amplitude of 5 mV.

1.5 Assembly of water-splitting electrolyzer

For testing in a AEMWE (Model: BKT2-SN-22-8X, manufactured by Jiangsu BOKE Co., Ltd., China), we prepared a AEMWE by sandwiching the Pt/C cathode and RuO_2/Co_3O_4 anode between a commercial membrane (Fumasep FAB-PK-130). In the AEMWE system, the 1.0 M KOH electrolyte is supplied to the cathode and anode at a flow rate of 40 mL min^{-1}. The

performance of the device is determined by measuring the LSV curve in the range 1.0 to 2.0 V, with a scan rate of 5 mV S^{-1}. To ensure the accuracy of the data, the performance test was performed three times to calculate the margin of error. For durability testing, AEMWE runs continuously with a peristaltic pump flow of 40 mL min^{-1} to circulate the electrolyte.

Supplementary figures

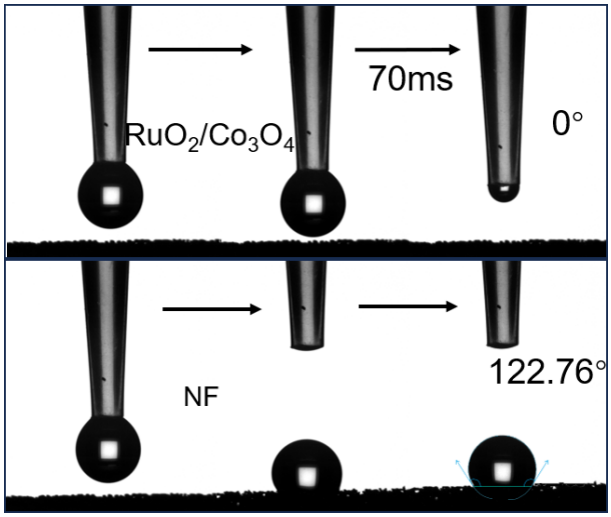

Fig. S1 Dynamic contact angle test of RuO_2/Co_3O_4 and NF.

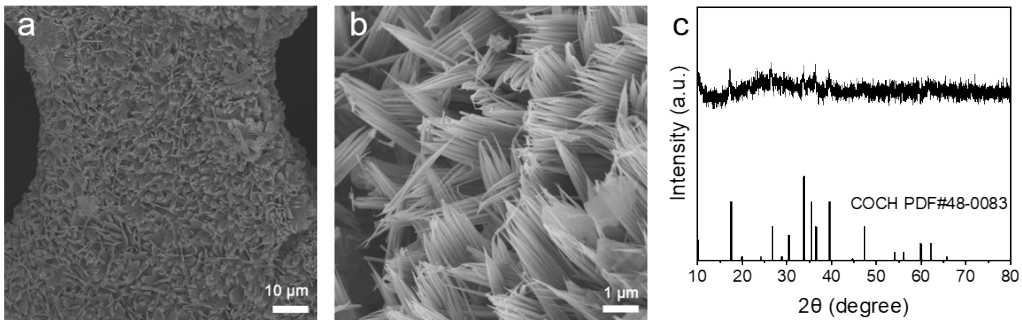

Fig. S2 (a-b) SEM images of CoCH. (C) XRD patterns of CoCH.

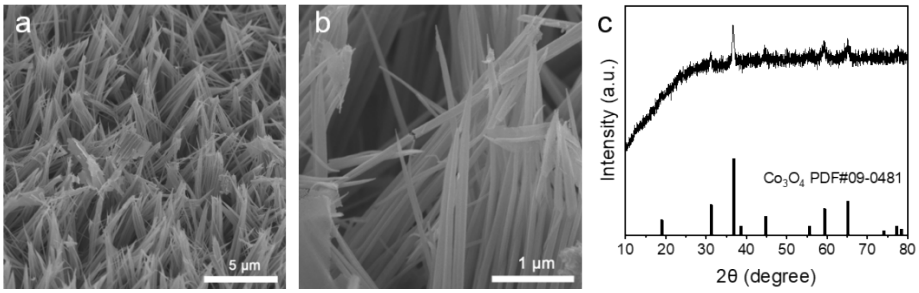

Fig. S3 (a-b) SEM images of RuO_2/Co_3O_4. (c) XRD patterns of Co_3O_4.

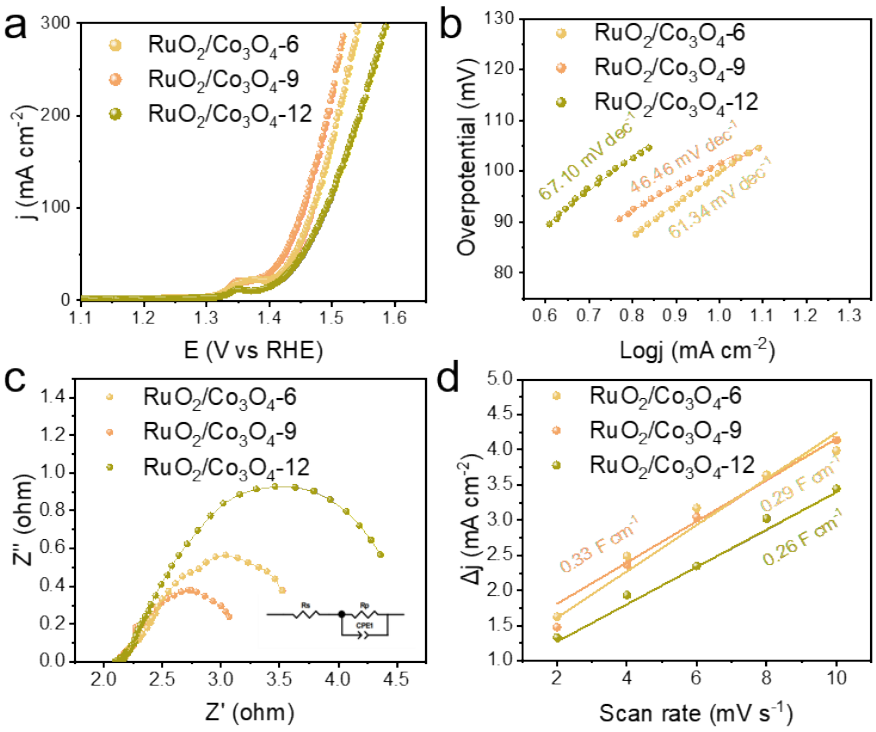

Fig. S4 (a) LSV curves, (b) corresponding Tafel slopes, (c) EIS Nyquist plots, (d) capacitive current density against the scan rate of RuO_2/Co_3O_4-6, RuO_2/Co_3O_4-9 and RuO_2/Co_3O_4-12.

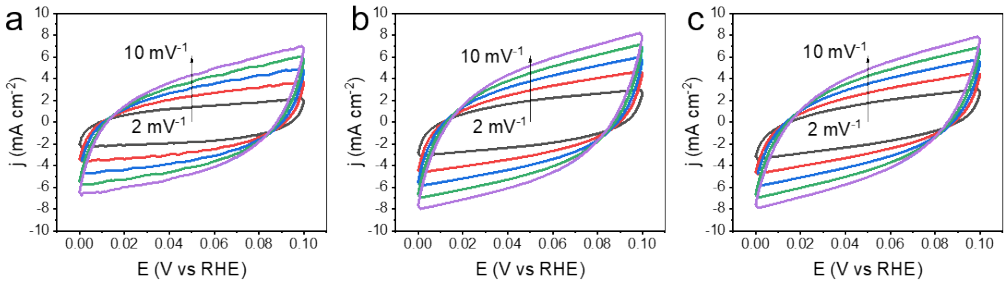

Fig. S5 CV curves of (a) RuO_2/Co_3O_4-6, (b) RuO_2/Co_3O_4-9 and (c) RuO_2/Co_3O_4-12.

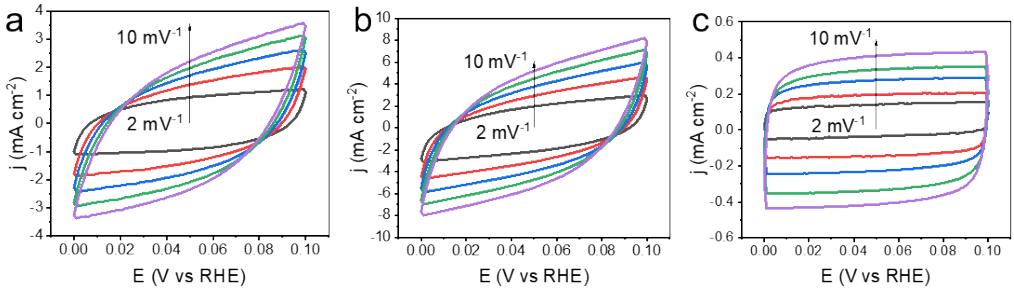

Fig. S6 CV curves of (a) Co_3O_4, (b) RuO_2/Co_3O_4-9 and (c) com. RuO_2.

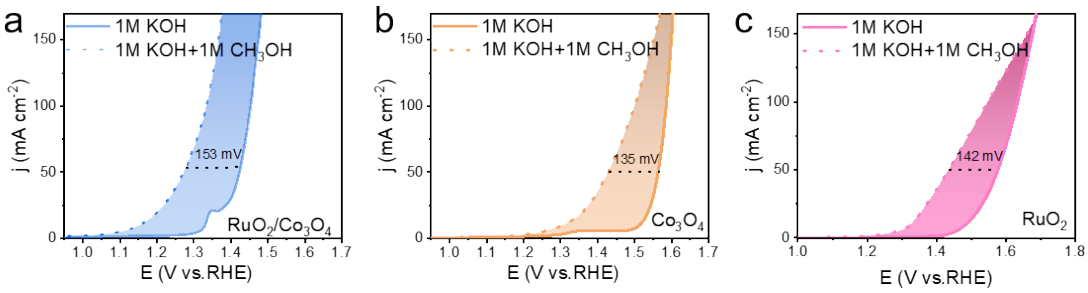

Fig. S7 Polarization curves of (e) RuO_2/Co_3O_4, (b) Co_3O_4 and (f) com. RuO_2 in 0.5 M KOH solution with (dashed lines) and without (solid lines) 1 M methanol.

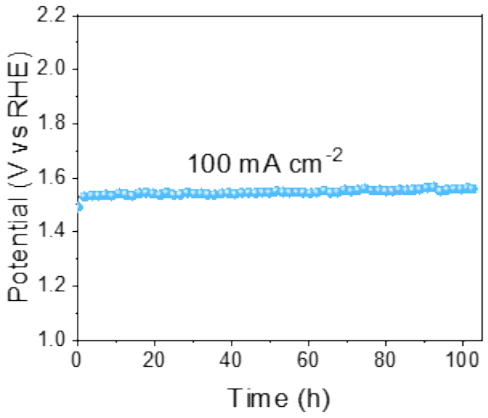

Fig. S8 The CP curves of RuO_2/Co_3O_4 operated at 100 mA cm^{-2}.

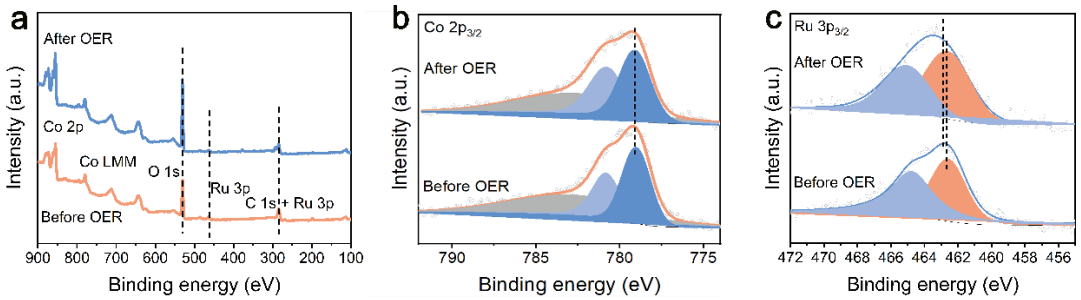

Fig. S9 (a) The whole XPS spectra, (b) Co $2p_{3/2}$, (c) Ru $3p_{3/2}$ XPS spectra of RuO_2/Co_3O_4 before and after stability test.

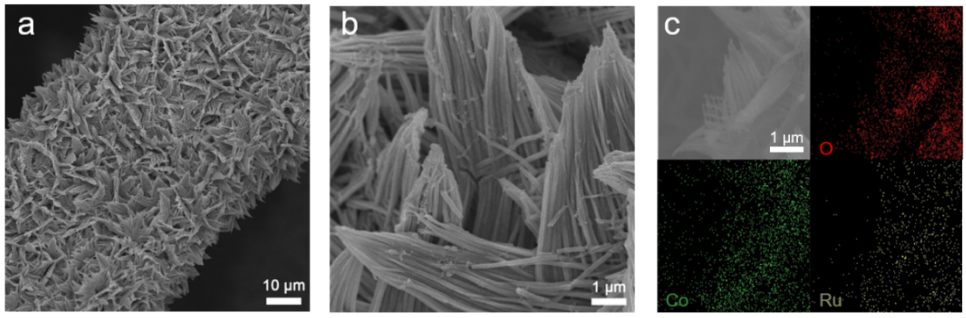

Fig. S10 (a-b) SEM, and (c) EDX mapping images of RuO_2/Co_3O_4 after stability test.

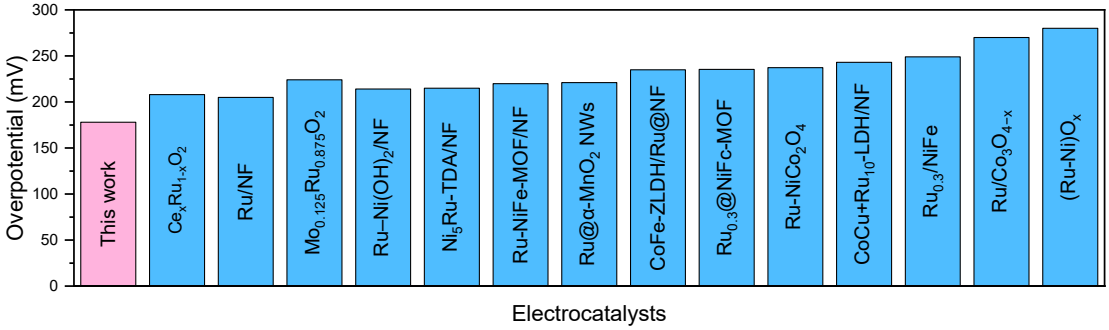

Fig. S10 Comparison of the OER overpotentials (at 10 mA cm^{-2}) of the RuO_2/Co_3O_4 with recently reported Ru-based electrocatalysts.

Table S1 The ruthenium loads in samples with different ion exchange times were determined by ICP-OES analysis.

Catalyst	Ru (wt%)	Co (wt%)
RuO_2/Co_3O_4-6	13.8	86.2
RuO_2/Co_3O_4-9	17.5	82.5
RuO_2/Co_3O_4-12	20.4	79.4

Catalyst	η at 10 $mA \cdot cm^{-2}$	Reference
$Ce_xRu_{1-x}O_2$	208	Ref. S1
Ru/NF	202	Ref. S2
Mo0.125Ru0.875O2	224	Ref. S3
Ru–$Ni(OH)_2$/NF	210	Ref. S4
Ni_5Ru-TDA/NF	215	Ref. S5
Ru-NiFe-MOF/NF	219	Ref. S6
Ru@α-MnO_2 NWs	221	Ref. S7
CoFe-ZLDH/Ru@NF	235	Ref. S8
$Ru_{0.3}$@NiFc-MOF	235	Ref. S9
Ru-$NiCo_2O_4$	237	Ref. S10
CoCu+Ru_{10}-LDH/NF	243	Ref. S11
$Ru_{0.3}$/NiFe	249	Ref. S12
Ru/Co_3O_{4-x}	270	Ref. S13
(Ru-Ni)O_x	280	Ref. S14

Table S2 Comparison of OER activities of recently reported electrocatalysts containing Ru.

References

1 P. Wang, J. Mu, G. Feng, Y. Fan, Y. Pan, L. Diao, Z. Miao and J. Zhou, *Chem. Commun.*, 2025.

2 Y. Hou, Z. Qin, X. Han, Y. Liu, W. Zhang, X. Cao, Y. Cao, J.-P. Lang and H. Gu, *Nanoscale*, 2024, **16**, 6662–6668.

3 Y. Liu, R. Deng, Y. Song, W. Tan, X. Tao, S. Luo, D. Long, S. Chen and Z. Wei, *Chem. Commun.*, 2025, **61**, 4547–4550.

4 C. Li, B. Kim, Z. Li, R. Thapa, Y. Zhang, J. Seo, R. Guan, F. Tang, J. Baek, Y. H. Kim, J. Jeon, N. Park and J. Baek, *Adv. Mat.*, 2024, **36**, 2403151.

5 J. Lin, H. Wang, C. Wang, L. Guo and Y. Wang, *Electrochim. Acta*, 2023, **470**, 143300.

6 W. Jiang, J. Wang, Y. Jiang, Y. Wu, B. Liu, X. Chu, C. Liu, G. Che and Y. Lu, *J. Mater. Chem. A*, 2023, **11**, 2769–2779.

7 N. Li, A. Yang, M. Jin, S. Wang, P. Yu, J. Wang and H. Jin, *Chem. Commun.*, 2025, **61**, 2762–2765.

8 H. Wang, Y. Zhang, G. Wu, L. Guo and Y. Wang, *Int. J. of Hydrogen Energy*, 2024, **64**, 261–268.

9 T. Liu, Y. Guan, Y. Wu, X. Chu, B. Liu, N. Zhang, C. Liu, W. Jiang and G. Che, *Int. J. of Hydrogen Energy*, 2024, **57**, 408–419.

10 Y. Wang, L. Chen, H. Zhang, M. Humayun, J. Duan, X. Xu, Y. Fu, M. Bououdina and C. Wang, *Green Chem.*, 2023, **25**, 8181–8195.

11 Y. Wang, L. Jing, W. Jiang, Y. Wu, B. Liu, Y. Sun, X. Chu and C. Liu, *J. of Colloid and Interface Sci.*, 2024, **671**, 283–293.

12 H. Xu, G. Xin, W. Hu, Z. Zhang, C. Si, J. Chen, L. Lu, Y. Peng and X. Li, *Appl. Catal. B Environ.*, 2023, **339**, 123157.

13 C.-Z. Yuan, S. Wang, K. San Hui, K. Wang, J. Li, H. Gao, C. Zha, X. Zhang, D. A. Dinh, X.-L. Wu, Z. Tang, J. Wan, Z. Shao and K. N. Hui, *ACS Catal.*, 2023, **13**, 2462–2471.

14 H. Zhang, Y. Lv, C. Chen, C. Lv, X. Wu, J. Guo and D. Jia, *Appl. Catal. B Environ.*, 2021, **298**, 120611.